

# Ion conduction mechanism in non-aqueous polymer electrolytes based on oxalic acid: Effect of plasticizer and polymer

Harinder Pal Singh Missan<sup>a</sup>, P.P. Chu<sup>a</sup>, S.S. Sekhon<sup>b,\*</sup>

<sup>a</sup> Department of Chemistry, National Central University, Chungli 32001, Taiwan

<sup>b</sup> Department of Applied Physics, Guru Nanak Dev University, Amritsar, Punjab 143005, India

Received 21 June 2005; accepted 20 October 2005

Available online 28 November 2005

## Abstract

Non-aqueous proton-conducting polymer electrolytes in the film form are synthesized through the complexation of oxalic acid (OA) and polyvinylidene fluoride-co-hexafluoro propylene (PVdF-HFP). Interestingly, the addition of a small amount of the basic component dimethylacetamide (DMA) gives rise to a three-order increase in conductivity. The value is found to depend on the concentrations of the weak acid and DMA in the electrolytes. A maximum conductivity of  $0.12 \times 10^{-3} \text{ S cm}^{-1}$  has been achieved at ambient temperature for electrolytes containing 40 wt.% OA with DMA. The observed increase in conductivity is considered to be due to interactions taking place between the high dielectric polymer media, the acid and the basic plasticizer. These interactions are confirmed from fourier transform infra red (FTIR) studies and supported by differential scanning calorimetry (DSC) measurements. Apart from providing acid–base interaction, the base DMA also improves the surface morphology and reduces the pore volume, both of which help to retain the acid–base complex within the membrane.

© 2005 Elsevier B.V. All rights reserved.

PACS: 73.61.Ph; 78.30.Jw; 82.45.Gj

Keywords: Ionic conductivity; Acid–base interaction; Oxalic acid; Ion aggregates; Polymer electrolyte; Solid-state battery

## 1. Introduction

Polymer electrolytes obtained by the complexation of metal salts with polyethylene oxide (PEO) have been widely studied for their application in solid-state batteries and other devices [1–6]. Nuclear magnetic resonance (NMR) and thermal studies show that PEO-based polymer electrolytes are multiphase materials with an amorphous phase responsible for high ionic conductivity [7]. An increase in the amorphous content of such polymer electrolytes by the addition of different plasticizers has been reported to result in an increase in conductivity [8–10]. Excessive use of plasticizer, however, decreases the dimensional stability of the membrane. Although much of the initial work was performed with different alkali metal salts due to their suitability as electrolytes in high-energy lithium polymer batteries, proton-conducting polymer electrolytes containing

different proton conductors also received attention [11–14]. The interest in these materials is mainly to develop non-aqueous proton-conducting membranes suitable for use in polymer electrolyte membrane fuel cells (PEMFCs). The low proton conductivity in these electrolytes generally limits their use in practical applications and an increase in conductivity to a value approaching  $10^{-3} \text{ S cm}^{-1}$  at room temperature is desirable [15].

The most widely used membranes in fuel cells today are based on a perfluorinated backbone with sulfonated side chains, e.g., Nafion. Despite its good performance in practical fuel cell conditions, Nafion has several disadvantages such as a workable temperature below  $100^\circ\text{C}$ , a high cost, and cross-over of methanol at high methanol concentration. Improved membranes should provide a wide-temperature workability, good stability towards harsh fuel cell environments and, above all, enhanced proton conductivity. An acid–base approach is one such attempt to realize high conductivity in the non-aqueous (polymer) form. Strongly bonded acid–base systems lead to brittle film formation, whereas weakly-bonded acid–base complexes display

\* Corresponding author. Tel.: +91 183 2711098; fax: +91 183 2258820.  
E-mail address: [sekhon\\_apd@yahoo.com](mailto:sekhon_apd@yahoo.com) (S.S. Sekhon).

flexural properties and can be employed to circumvent the brittleness issue [16–19]. The objective of the present work is to investigate the synthesis of the membranes based on a weak acid–base system and to understand the effect of the addition of weak base on the electrical, morphological and thermal properties.

The present study examines polymer electrolyte membranes that contain polyvinylidene fluoride-co-hexafluoropropylene (PVdF-HFP), which is an amorphous polymer, and oxalic acid, which is a weak dicarboxylic acid (COOH–COOH) (OA) with a dissociation constant of  $5.4 \times 10^{-2}$  (in aqueous solution). Dimethylacetamide (DMA) with a dielectric constant ( $\epsilon = 37.8$ ) that is higher than that of PVdF-HFP ( $\epsilon = 7.8$ ) is used as a basic plasticizer. Weak acid–base interaction is essential for proton conduction in a non-aqueous medium. The variation of conductivity of non-aqueous electrolytes with acid concentration, plasticizer and temperature is presented. The various levels of structural characteristics resulting from the addition of the basic component are also examined by use of fourier transform infra red spectroscopy (FTIR), differential scanning calorimetry (DSC), thermogravimetric analysis (TGA) and scanning electron microscopy (SEM).

## 2. Experimental

Polyvinylidene fluoride-co-hexafluoropropylene (PVdF-HFP) (Fluka,  $M_w = 1.3 \times 10^5$ ), oxalic acid (OA) (Qualigen, AR), dimethylacetamide (DMA) (Merck) and tetrahydrofuran (THF) (Merck) were used as the starting materials in the preparation of polymer electrolytes by a solution-casting method. Films of PVdF-HFP-OA were obtained by dissolving PVdF-HFP and OA in stoichiometric quantities (expressed as weight percentage of the polymer) in THF to obtain a uniform solution. To obtain acid–base based electrolyte films, DMA in different proportions (expressed as the weight percentage of the polymer electrolyte) was also added. The mixture was stirred and a clear, homogenous and viscous solution was obtained that was then poured into polypropylene dishes and the solvent was allowed to evaporate slowly in a vacuum oven. The films so prepared were found to be mechanically stable and transparent with a thickness  $\sim 100 \mu\text{m}$ . The electrical conductivity of the films was measured by means of a HP4284A precision LCR meter in the frequency range 20 Hz–1 MHz by the method described earlier [14]. The FTIR measurements were carried out at room temperature using a Perkin-Elmer FTIR spectrometer in the 400–4000  $\text{cm}^{-1}$  range. Differential scanning calorimetry (DSC) experiments were carried out using Perkin-Elmer (DSC 7 series) equipment in the temperature range  $-60$  to  $200^\circ\text{C}$  at a scan rate of  $10^\circ\text{C min}^{-1}$  in a flow of nitrogen gas. The weight of the sample was maintained at 3–5 mg for all experiments. Thermal gravimetric analysis (TGA) studies were performed with Perkin-Elmer (TGA 7 Series) equipment over the temperature range 20– $900^\circ\text{C}$  and at rate of  $10^\circ\text{C min}^{-1}$  in a flow of nitrogen gas. The surface morphologies of these electrolytes were studied by means of a LV-Scanning Electron Microscope (LV-SEM) model Hitachi 3500N.

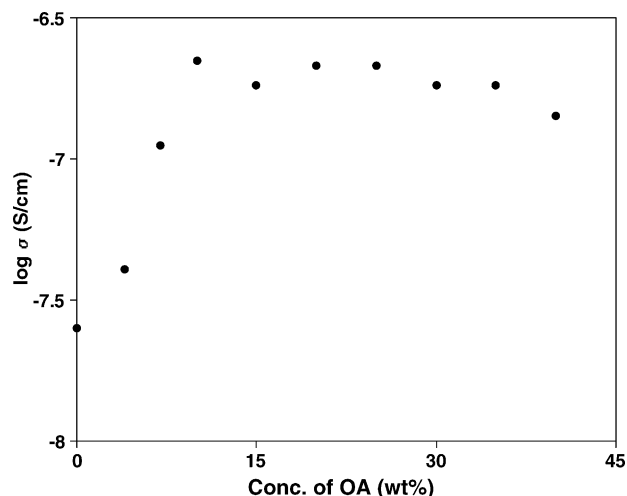


Fig. 1. Variation of conductivity of (PVdF-HFP)-OA polymer electrolytes with concentration of OA.

## 3. Results and discussion

The variation of the conductivity of (PVdF-HFP)-OA polymer electrolytes with OA concentration (expressed as wt.% of polymer) is given in Fig. 1. At low OA concentrations, the conductivity increases with increase in acid concentration. After reaching the maximum value of  $2.2 \times 10^{-7} \text{ S cm}^{-1}$  (i.e., for a polymer electrolyte containing 10 wt.% oxalic acid), the conductivity appears saturated with further increase in acid concentration. The low value of conductivity may be due to the low dissociation constant of OA. The initial increase could be due to the dissociation of the acid that arises from the interaction between the acid and the polymer. The saturation observed at higher acid concentrations could be due to the formation of ion aggregates, which do not contribute to the conductivity. The increase in acid concentration also leads to an increase in viscosity due to the interactions between acid and polymer. This lowers mobility and the conductivity decreases.

The formation of ion aggregates in polymer electrolytes at higher acid concentrations has been substantiated by: (i) mass action considerations [20]; (ii) impedance spectroscopy; (iii) FTIR measurements. According to simple mass action considerations, the presence of ion aggregates can be estimated from the nature of a  $\log \sigma$  versus  $\log C$  plot, where  $\sigma$  is the conductivity and  $C$  is the concentration of salt or acid in the electrolyte. A linear plot implies that ion aggregation is unimportant, while any deviation from linear behaviour indicates the presence of ion aggregates. This method has been successfully used earlier to study the presence of ion aggregates in PEO-based polymer electrolytes [21–22]. The plot of  $\log \sigma$  versus  $\log C$  for (PVdF-HFP)-OA polymer electrolytes is given in Fig. 2. A linear plot is clearly observed at low acid concentrations (0–10 wt.%) but a large deviation from a straight line occurs at higher acid concentrations (15–40 wt.%). Clearly, this suggests the presence of ion aggregates at higher acid concentrations.

As DMA has a basic nature and a dielectric constant that is higher than that of PVdF-HFP, it was used as a plasticizer in a blend with polymer electrolytes containing 30 wt.% OA.

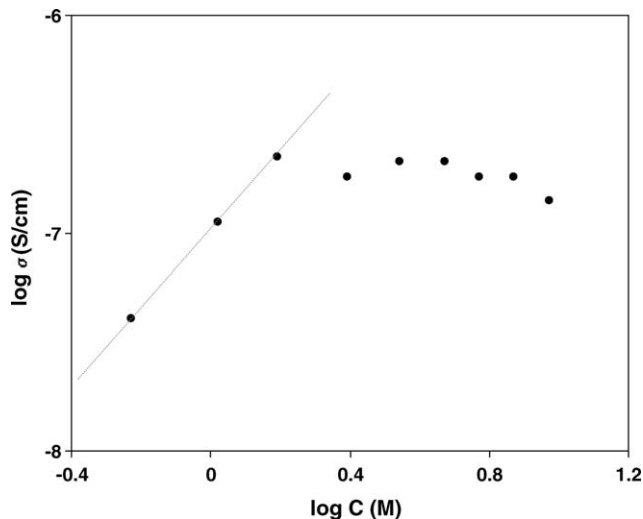


Fig. 2. Variation of  $\log \sigma$  with  $\log C$  for (PVdF-HFP)-OA polymer electrolytes.

This composition was chosen because it contains ion aggregates/undissociated acid as evident from the data given in Figs. 1 and 2. The variation of conductivity of (PVdF-HFP)-OA as a function of DMA concentration (expressed as wt.% of polymer electrolyte) was also studied and the results are presented in Fig. 3. It can be seen that the conductivity increases continuously with an increase in DMA concentration and reaches a maximum value of  $4.2 \times 10^{-5} \text{ S cm}^{-1}$ . The amount of DMA was limited to 43 wt.% since the film suffers degradation in its mechanical properties and becomes sticky above this concentration. This observation is in sharp contrast with the traditional understanding that an acid with a higher acidity constant or a large amount of acid in the electrolytes is required to raise the proton conductivity as it increases the number of free ions for conduction. In present study, we have used a weak acid, whose dissociation constant is substantially lower than unity and upon the addition of a small amount of basic plasticizer, a three-fold increase in the conductivity is observed. As will be demonstrated, the increase

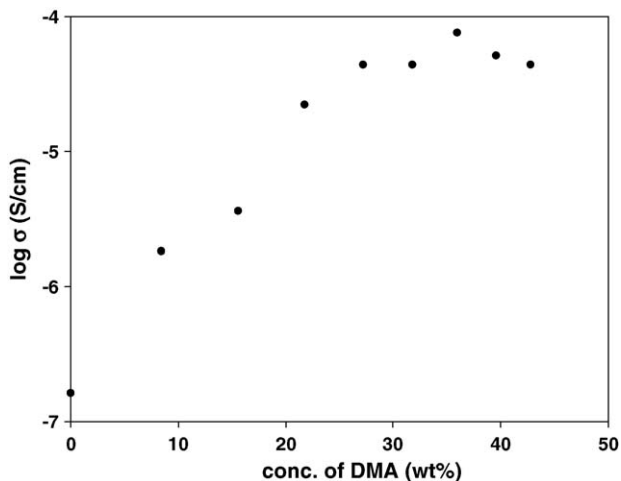


Fig. 3. Effect of addition of DMA on conductivity of (PVdF-HFP)-OA polymer electrolytes.

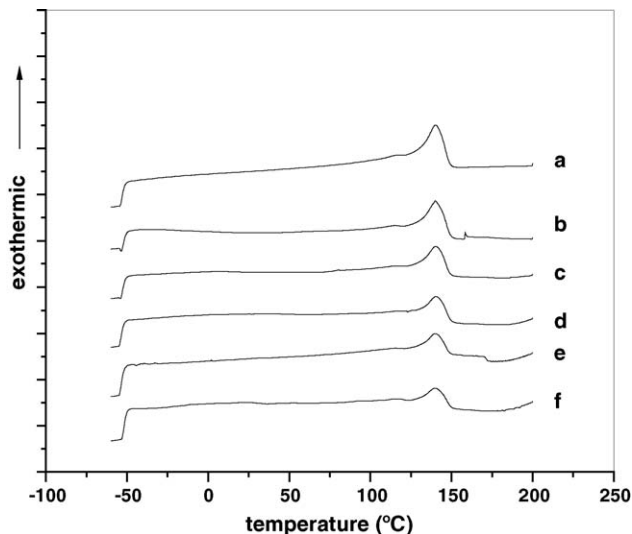


Fig. 4. DSC thermograms of (PVdF-HFP)-OA polymer electrolytes ((a) 0, (c) 20 and (e) 40 wt.% OA), and (PVdF-HFP)-OA-DMA polymer electrolytes with (b) 0, (d) 20 and (f) 40 wt.% OA and containing 36 wt.% DMA.

could be accountable by improved proton dissociation due to the formation of acid–base interactions.

The polymer (PVdF-HFP) used in the present study is highly amorphous so that the addition of DMA as a plasticizer does not substantially increase the amorphous content. This was checked experimentally from DSC thermograms in the temperature range of  $-60$  to  $200$  °C and is shown in Fig. 4. The characteristics evaluated from DSC measurements are listed in Table 1. Usually, the addition of plasticizer leads to the interruption of polymer crystallization and an increase in the amorphous content. In the present investigation, however, the DSC results indicate there is no substantial change in the crystallinity of the polymer electrolytes with the addition of DMA, but a large decrease in crystallinity is found with the addition of 20–40 wt.% OA. By contrast, there is a substantial increase in the conductivity with the addition of DMA, but not with the OA. Therefore, it can be concluded that the increase in ion conductivity must be due to improved dissociation that results from acid–base interactions taking place between OA and DMA, and not due to a change of crystallinity. In accord with this conclusion is the observation that a greater increase in conductivity with the addition of DMA is found at higher concentrations of OA, since the amount of undissociated acid will increase as the OA content is increased. The trends in the change of crystallinity also suggests a more

Table 1  
Summary DSC data

Sample code <sup>a</sup>	$T_c$ (°C)	$T_m$ (°C)	$\Delta H$ (J g <sup>-1</sup> )	Crystallinity (%)
PH	113.6	140.2	23.06	100
PHD	112.8	139.9	13.09	98
PH20A	113.1	140.6	9.90	81
PH20AD	112.9	140.6	9.14	74
PH40A	113.1	139.9	6.97	55
PH40AD	112.7	139.9	6.93	57

<sup>a</sup> PH: PVdF-HFP; 20A and 40A: 20 and 40 wt.% oxalic acid, respectively; D: 36 wt.% DMA.

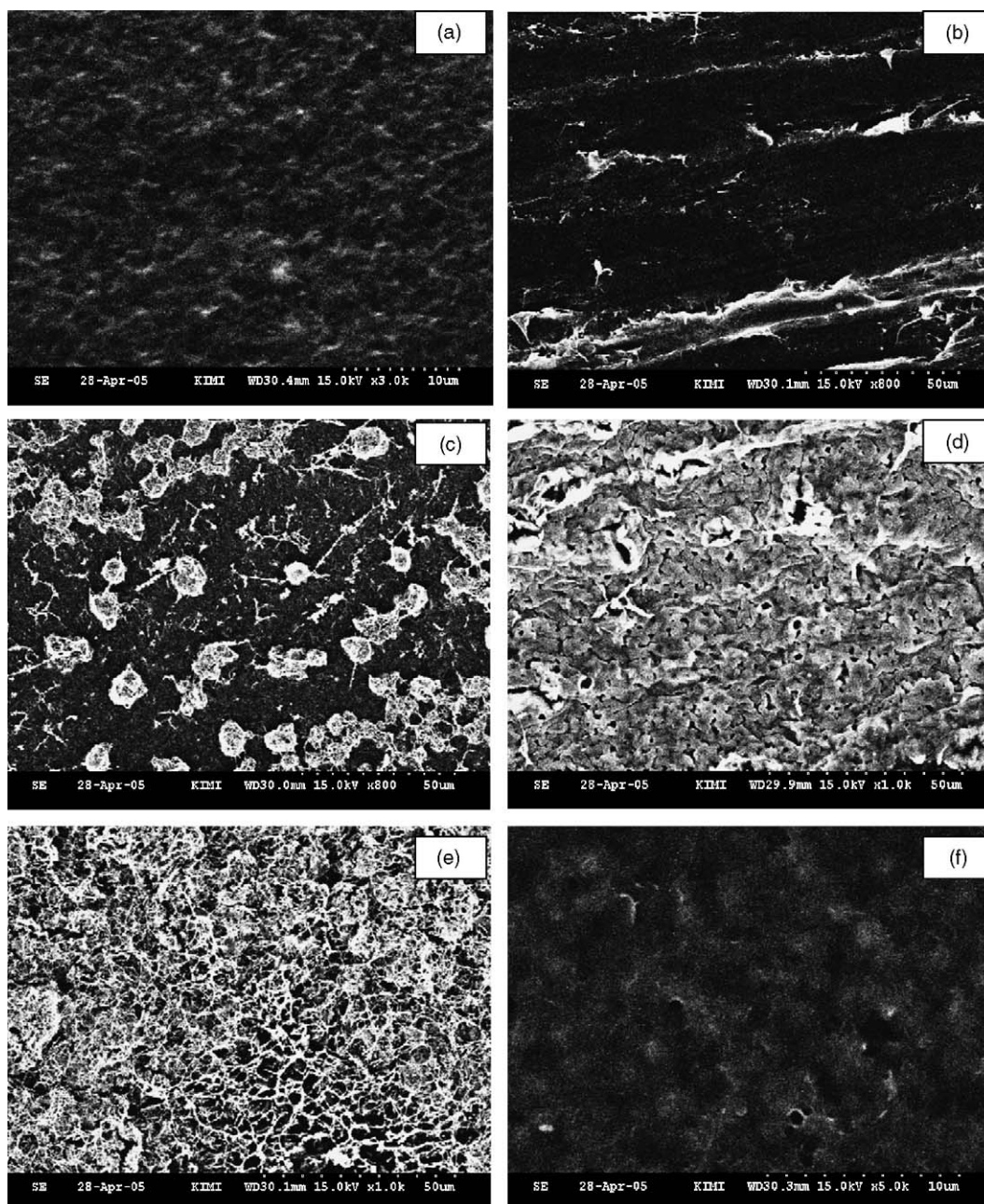


Fig. 5. Scanning electron micrographs for (PVdF-HFP)-OA polymer electrolytes containing (a) 0, (c) 20 and (e) 40 wt.% OA without DMA and corresponding (PVdF-HFP)-OA-DMA polymer electrolytes with (b) 0, (d) 20 and (f) 40 wt.% OA containing 36 wt.% DMA.

intimate interaction of OA with PVdF-HFP which is sufficient to interrupt PVdF-HFP crystallization. This is less than between DMA and PVdF-HFP. The difference can be easily justified by the formation of hydrogen bonding between OA and the fluorine in PVdF-HFP (*vide infra*).

Apart from contributing to acid–base interactions, DMA also plays an important role in improving the morphology of the electrolyte, as observed from SEM studies. Fig. 5 shows the electron micrographs of PVdF-HFP-OA-based polymer electrolyte containing (a) 0, (c) 20, and (e) 40 wt.% OA and their corresponding polymer electrolytes with (b) 0, (d) 20 and (f) 40 wt.% OA and containing 36 wt.% DMA. It is found that the films containing 40 wt.% OA shows an improved morphology. Moreover, still

further improvement in the morphology can be observed with the addition of DMA. In fact, the film with 40 wt.% OA and DMA is the best homogeneously distributed system.

In order to provide further evidence of the interactions/complexation between acid, polymer and DMA for polymer electrolytes with DMA and without DMA, FTIR spectroscopic studies were conducted at room temperature. For all samples, the spectra were recorded in the  $4000\text{--}400\text{ cm}^{-1}$  region under similar conditions. Spectra in the  $400\text{--}1600\text{ cm}^{-1}$  range for (PVdF-HFP)-OA (with and without DMA) polymer electrolytes containing 0, 20 and 40 wt.% oxalic acid are given in Fig. 6. These compositions have been chosen because they contain different levels of acid–base interaction as explained

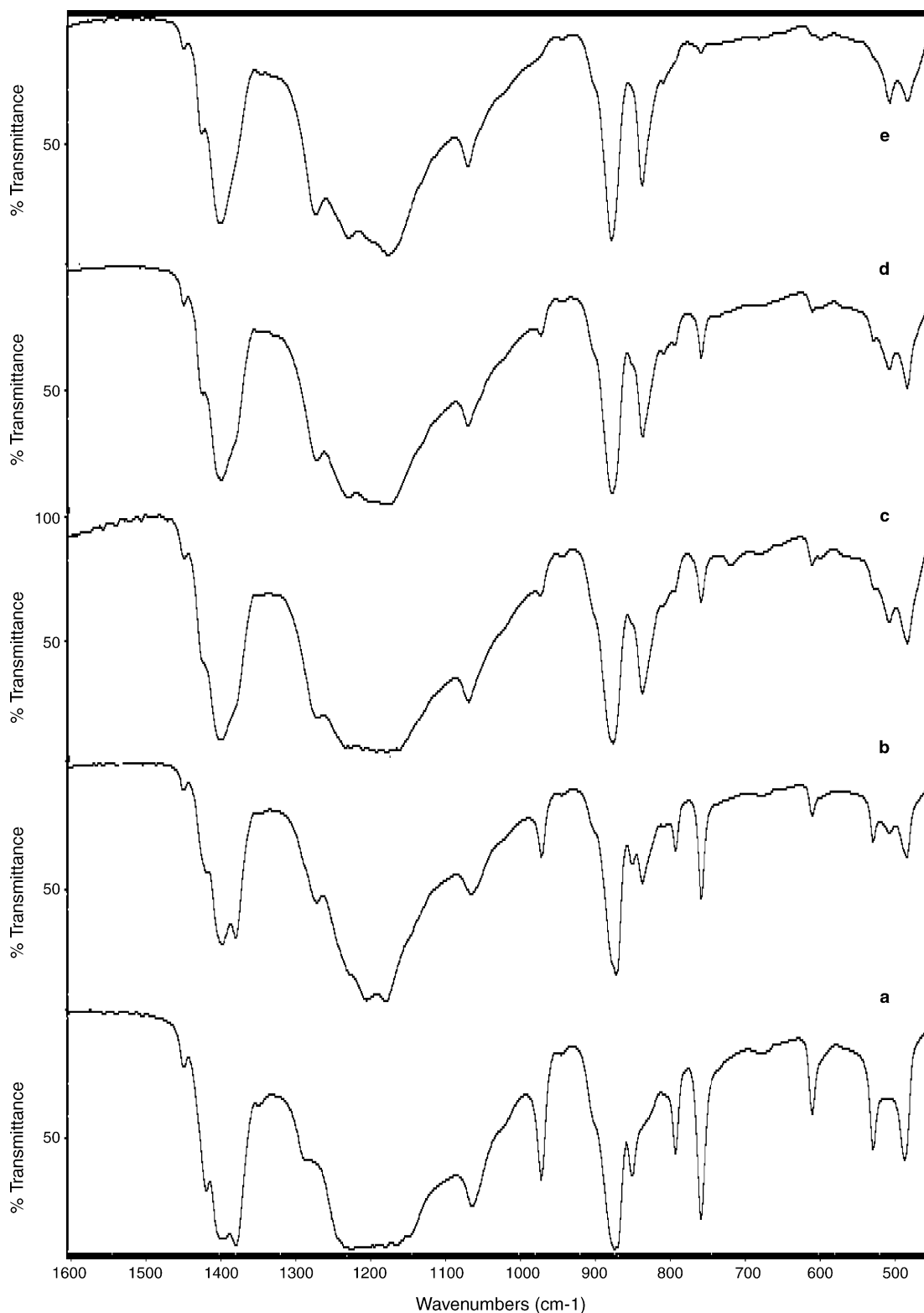


Fig. 6. FTIR spectra of (PVdF-HFP)-OA polymer electrolytes containing (a) 0, (b) 20 and (d) 40 wt.% OA without DMA and (PVdF-HFP)-OA-DMA, polymer electrolytes with (c) 20 and (e) 40 wt.% OA and containing 36 wt.% DMA.

previously in Figs. 1 and 2. It is clear that the spectrum of PVdF-HFP (Fig. 6(a)) in the 400–1000  $\text{cm}^{-1}$  range contains peaks at wavenumbers 489, 531, 613, 761, 796, 854, 877 and 975  $\text{cm}^{-1}$  that corresponds to vinylidene, C–F deforma-

tion, methylene rocking,  $\text{CH}_2$  wagging of the vinylidene band and out-of-plane C–H stretching, respectively [23–24]. With the addition of 20 wt.% OA to PVdF-HFP, the FTIR spectrum (Fig. 6(b)) undergoes significant changes and the intensities of

all the above-mentioned peaks decrease. When the OA concentration is increased to 40 wt.% (Fig. 6(d)), the intensities of above peaks decrease further so that the peaks at wavenumbers 531, 613, 796 and 975  $\text{cm}^{-1}$  almost become shoulders while the peak at 854  $\text{cm}^{-1}$  disappears. Some new peaks are also observed at wavenumbers 512 and 840  $\text{cm}^{-1}$  with the addition of OA and their intensities increase with an increase in OA concentration from 20 to 40 wt.%. Similarly the FTIR spectra of these polymer electrolytes in the 1300–1500  $\text{cm}^{-1}$  region show that PVdF-HFP contains peaks at 1383, 1401, 1423 and 1453  $\text{cm}^{-1}$  that are associated with scissoring vibration of the vinyl group and C–H rocking vibrations. The intensity of these peaks changes on the addition of 20 wt.% OA and polymer electrolytes containing 40 wt.% OA show that the peak at 1383  $\text{cm}^{-1}$  becomes a weak shoulder whereas the intensity of other peaks decreases. The above results indicate that interactions of OA with PVdF-HFP are taking place.

These observed changes in the FTIR spectra of PVdF-HFP on the addition of OA can be explained as follows. The peaks associated with the vinylidene group of the polymer at positions 489, 531, 613, 796, 875  $\text{cm}^{-1}$  exhibit a slight change in position together with a reduction in intensity. The relative intensities of the PVdF-HFP peaks at 1383 and 1401  $\text{cm}^{-1}$  (the 1383 peak is more intense than the 1402 peak) reverses for 20 wt.% OA. At 40 wt.% OA, the 1383 peak changes to a weak shoulder and the 1401 peak dominates. These peaks are also related to the vinyl groups of PVdF-HFP and therefore suggests that interaction takes place between the polymer and the acid. This result concurs with the DSC measurement. It is plausible that the free  $\text{H}^+$  ions interact with the electronegative fluorine of the trisubstituted vinylidene ( $\text{CF}_3$ ) group in PVdF-HFP. These peaks appear when OA is added to PVdF-HFP and their intensity increases with increase in OA concentration, as shown in Fig. 6.

The conductivity enhancement of (PVdF-HFP)-OA polymer electrolytes by the addition of DMA (as demonstrated in Fig. 3) has also been studied by FTIR. The FTIR spectra of PVdF-HFP + OA polymer electrolytes with 20 wt.% and with 40 wt.% OA and each containing 36 wt.% DMA are presented in Fig. 6(c) and (e), respectively. The data in Fig. 6 has shown that the spectrum of a polymer electrolyte containing 20 wt.% OA with DMA is quite similar to the spectrum of a polymer electrolyte containing 40 wt.% OA without DMA. In earlier section, it was noted that with an increase in OA concentration from 20 to 40 wt.%, the intensities of peaks at 489, 531, 613, 796, 1383 and 1401  $\text{cm}^{-1}$  are decreased with some peaks reduced to a shoulder. This has been explained in terms of the availability of more free  $\text{H}^+$  ions at higher OA concentrations and that these ions interact with the vinylidene group of the polymer. The same results have now been obtained by keeping the concentration of OA at 20 wt.% but with adding DMA. The FTIR data also indicate that more free  $\text{H}^+$  ions are available on the addition of DMA and this is mainly due to the improved dissociation of acid from the weak acid–base interaction. The addition of DMA to polymer electrolytes containing 40 wt.% OA results in a further decrease in the intensity of the above-mentioned peaks and some of the peaks almost disappear. At a high OA concentration (40 wt.%), the amount of acid will be higher and dissociation with the addi-

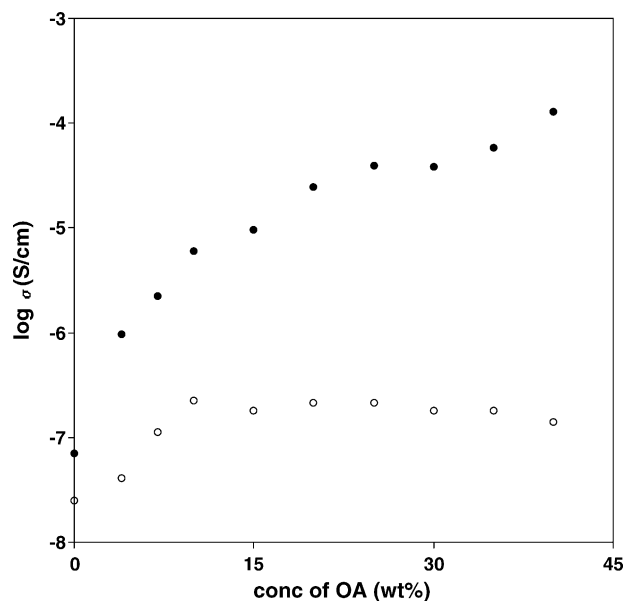


Fig. 7. Variation of conductivity with OA concentration for (○) (PVdF-HFP)-OA without DMA and (●) (PVdF-HFP)-OA-DMA polymer electrolytes containing 36 wt.% DMA.

tion of DMA results in more free  $\text{H}^+$  ions, which contribute to a more pronounced enhancement in conductivity. Thus, a probable mechanism for conduction in these electrolytes is the control of the movement of ions by both DMA and the polymer. This will lead to dissociation of the acid and also to the provision of channels for conduction that will result in more mobility and higher conductivity.

The effect of basic plasticizer (DMA) in improving the proton conductivity was evaluated by undertaking impedance spectroscopy measurements on samples that contained different concentrations of OA, i.e., different level of acid–base interaction. The same amount of DMA was added to the (PVdF-HFP)-OA polymer electrolytes that had different concentrations of OA (0–40 wt.%). The conductivity of the polymer electrolytes was measured as a function of OA concentration and the results are given in Fig. 7. For comparison, the variation of the conductivity of (PVdF-HFP)-OA electrolytes without DMA is also presented in Fig. 7. It is found that the increase in conductivity with DMA addition also depends on the concentration of acid present in the polymer electrolyte. The increase in conductivity with DMA addition is by one order of magnitude at low (0–10 wt.%) OA concentrations, by two orders of magnitude at medium (20–30 wt.%) acid concentrations, and by three orders of magnitude at higher (40 wt.%) OA concentrations. The relative increase in conductivity (expressed as  $\sigma/\sigma_0$ , where  $\sigma$  and  $\sigma_0$  are the conductivities of (PVdF-HFP)-OA-DMA containing DMA and (PVdF-HFP)-OA polymer electrolytes without DMA, respectively) has been calculated and is presented in Fig. 8 as a function of OA concentration. It is seen that the conductivity in the presence of DMA addition increases with increase in OA concentration.

The correlation between the increase in conductivity with DMA addition and the dissociation of acid was also examined in terms of mass action considerations, as given in Fig. 2. A plot

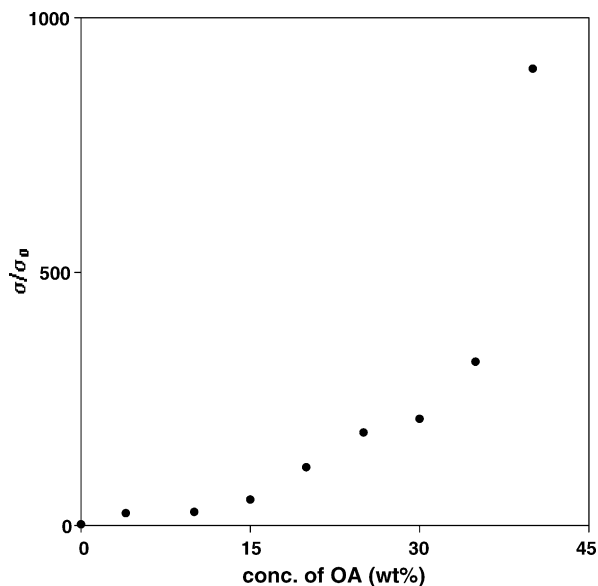


Fig. 8. Variation of relative increase in conductivity ( $\sigma/\sigma_0$ ) (where  $\sigma$  and  $\sigma_0$  are conductivities of polymer electrolytes with and without DMA, respectively) with OA concentration.

of  $\log \sigma$  versus  $\log C$  for polymer electrolytes with DMA is given in Fig. 9 together with the corresponding plot for polymer electrolyte without DMA. A nearly linear plot is found for polymer electrolytes with DMA. For electrolytes without DMA however, a linear relationship is observed only at low (0–10 wt.%) OA concentrations. This suggests that ion aggregates and undissociated acid are not present when DMA is added to the polymer.

Finally, TGA studies were carried out on samples containing 0, 20 and 40 wt.% OA with and without DMA; the results are given in Fig. 10. There is only a very small initial weight

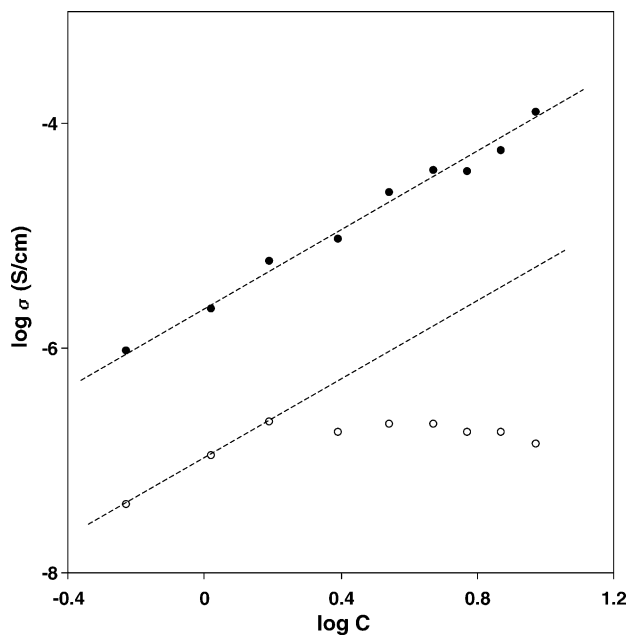


Fig. 9.  $\log \sigma$  vs.  $\log C$  for (○) (PVdF-HFP)-30 wt.% OA without DMA and (●) corresponding (PVdF-HFP)-OA-DMA polymer electrolytes with 36 wt.% DMA.

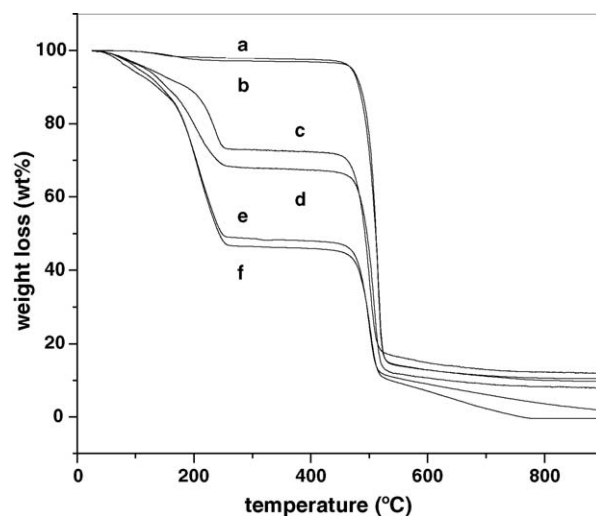


Fig. 10. TGA thermograms for (PVdF-HFP)-OA polymer electrolytes without DMA containing (a) 0, (c) 20 and (e) 40 wt.% OA and corresponding (PVdF-HFP)-OA-DMA polymer electrolytes with (b) 0, (d) 20 and (f) 40 wt.% OA containing 36 wt.% DMA.

loss for electrolytes containing 0 wt.% OA and this is possibly due to the evaporation of the solvent left in the electrolytes. The large decrease in weight at temperatures around 450 °C is due to decomposition of the polymer. With addition of 20 wt.% OA, the behaviour of electrolytes with and without DMA is very similar. A 7–8% weight loss is observed up to temperatures of 150 °C and this is probably due to solvent remaining in the electrolytes. The second weight decrease observed at temperature around 180–200 °C is due to evaporation of DMA, while the loss at around 450 °C results from decomposition of the polymer. A similar trend in behaviour is observed for electrolytes containing 40 wt.% OA. In summary, TGA studies show that these electrolytes preserve their composition and are stable up to 150 °C.

Conductivity cycling is a good indicator of the stability of the electrolyte. As shown in Fig. 11, the conductivity of polymer

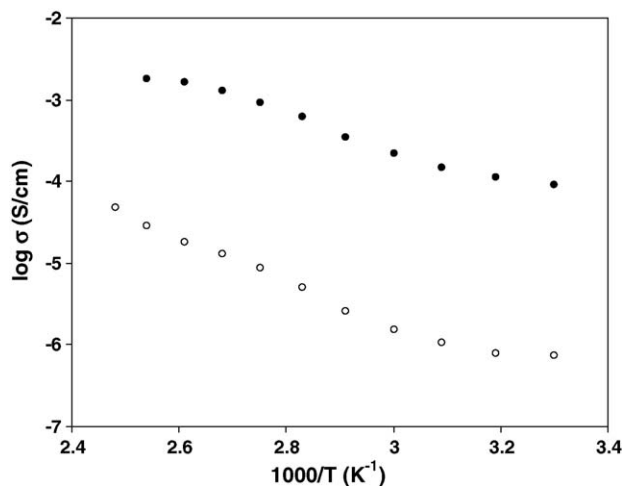


Fig. 11. Temperature dependence of conductivity of (○) (PVdF-HFP)-30 wt.% OA without DMA and (●) corresponding plasticized (PVdF-HFP)-OA-DMA polymer electrolytes containing 36 wt.% DMA.

electrolytes with DMA is about two orders of magnitude higher than that of polymers without DMA at all temperatures in the 300–400 K range. The slope of the plot, which can be described by a simple Arrhenius relationship, yields low activation energies of 0.15 eV (with DMA) and 0.2 eV (without DMA). These values are much lower than those for most proton conduction processes via vehicle mechanisms (0.3–0.4 eV) or for those assisted by polymer libration ( $\sim 0.5$  eV). Further work is in progress to define the conduction mechanisms taking place in the polymer systems that are being investigated here. The linear relationship suggests that polymer segmental motion is not playing a role in ion conduction. Conductivity data during cooling reproduces that found in the heating cycle (results of cooling cycle not shown) and this also suggests that there is no structure or composition variation in the electrolytes for temperatures up to 400 K. This feature is important for application of the non-aqueous polymer electrolyte systems in fuel cells that are operated at elevated temperatures (i.e., above 80 °C).

#### 4. Conclusions

Polymer electrolytes containing PVdF-HFP and oxalic acid have been prepared and are found to have low conductivities. The addition of DMA as a basic component (plasticizer) with dielectric constant higher than PVdF-HFP results in an increase in conductivity by nearly three orders of magnitude; a maximum conductivity of  $0.12 \times 10^{-3} \text{ S cm}^{-1}$  has been obtained. The increase in conductivity with DMA depends on the concentration of acid (OA) and plasticizer (DMA) in the polymer electrolytes. The effect is attributed to the dissociation of acid by the polymer and DMA due to acid–base interactions taking place between these components. This proposition is supported by FTIR studies. It is concluded that DMA and the polymer provide a combined conduction mechanism for proton transport. Both DSC and TGA studies demonstrate that the electrolytes are stable up to 150 °C. The addition of the basic component DMA is also found to change the morphology of the electrolytes.

#### Acknowledgements

The authors are grateful to Prof. S. Chandra (BHU) for his interest in the present work, to CSIR New Delhi for financial support in the form of research project No. 03(962)02/EMR II, and to RSIC, Punjab University Chandigarh for FTIR mea-

surements. Financial support from the National Science Council (Taiwan) under contract No. NSC 94-2811-M-008-008 is also acknowledged.

#### References

- [1] M.B. Armand, J.M. Chabagno, M.J. Duclot, in: P. Vashishta, J.N. Mundy, G.K. Shenoy (Eds.), *Fast Ion Transport in Solids*, North Holland, New York, USA, 1979, pp. 131–133.
- [2] J.R. MacCallum, C.A. Vincent, *Polymer Electrolyte Reviews*, vols. 1–2, Elsevier Applied Science, London, UK, 1987, 1989.
- [3] R.G. Linford, *Electrochemical Science and Technology of Polymers* vols. 1–2, Elsevier Applied Science, London, UK, 1987, 1990.
- [4] R. Koksang, I.I. Olsen, D. Shackle, *Solid State Ionics* 69 (1994) 320–335.
- [5] N. Choi, J. Park, *Electrochim. Acta* 46 (2001) 1453–1459.
- [6] F.M. Gray, *Polymer Electrolytes*, Royal Society of Chemistry, London, UK, 1997.
- [7] C. Berthier, W. Gorecki, M. Minier, M.B. Armand, J.M. Chabagno, P. Rigaud, *Solid State Ionics* 11 (1983) 91–95.
- [8] C.D. Robitaille, D. Fauteux, *J. Electrochem. Soc.* 133 (1986) 315–321.
- [9] K.M. Abraham, Z. Jiang, B. Carroll, *Chem. Mater.* 9 (1997) 1978–1988.
- [10] C. Booth, C.V. Nicholas, D.J. Wilson, in: J.R. MacCallum, C.A. Vincent (Eds.), *Polymer Electrolyte Reviews*, vol. 2, Elsevier Applied Science, London, UK, 1989, p. 229.
- [11] P. Colomban, *Proton Conductors: Solids, Membranes and Gels—Materials and Devices*, Cambridge University Press, Cambridge, UK, 1992.
- [12] S. Chandra, K.K. Maurya, S.A. Hashmi, in: B.V.R. Chowdari, Q. Liu, L. Chen (Eds.), *Recent Advances in Fast Ion Conducting Materials and Devices*, World Scientific, Singapore, 1990, p. 549.
- [13] H.S. Lee, X.B. Yang, J. McBreen, Z.S. Xu, T.A. Skotheim, Y. Okamoto, *J. Electrochem. Soc.* 141 (1994) 886–891.
- [14] M. Kumar, S.S. Sekhon, *Eur. Polym. J.* 38 (2002) 1297–1304.
- [15] B. Scrosati (Ed.), *Applications of Electroactive Polymers*, Chapman and Hall, London, UK, 1993.
- [16] J. Kerres, A. Ullrich, F. Meier, T. Haring, *Solid State Ionics* 125 (1999) 243–249.
- [17] J. Kerres, A. Ullrich, T. Haring, M. Baldauf, U. Gebhardt, W. Preidel, *J. New Mater. Electrochem. Syst.* 3 (2000) 129–239.
- [18] J. Roziere, D.J. Jones, *Ann. Rev. Mater. Res.* 33 (2003) 503–555.
- [19] L. Jorissen, V. Gogel, J. Kerres, J. Garche, *J. Power Sources* 105 (2002) 267–273.
- [20] M.A. Ratner, in: J.R. MacCallum, C.A. Vincent (Eds.), *Polymer Electrolyte Reviews*, vol. 1, Elsevier Applied Science, London, UK, 1989, p. 173.
- [21] A. Kallis, J.F. LeNest, A. Gadini, H. Cheradame, *Makromol. Chem.* 183 (1982) 2835–2839.
- [22] A. Kallis, J.F. LeNest, A. Gadini, H. Cheradame, *Macromolecules* 17 (1984) 63–66.
- [23] R.M. Silverstein, F.X. Webster, *Spectroscopic Identification of Organic Compounds*, sixth ed., John Wiley and Sons, New York, USA, 1997, Chapter 4.
- [24] G. Socrates, *Infrared and Raman Characteristic Group Frequencies: Tables and Charts*, second ed., Wiley Science, London, UK, 1998.